A Study of Electrochemical Reduction of Ethylene and Propylene Carbonate Electrolytes on Graphite Using ATR-FTIR Spectroscopy

Guorong V. Zhuang[a,*,z] Hui Yang[b,*], Berislav Blizanac[a],

and Philip N. Ross, Jr.[a,*]

Materials Sciences Division[a] and Environmental Energy Technologies Division[b]

Lawrence Berkeley National Laboratory

Berkeley, CA 94720

Abstract

We present results testing the hypothesis that there is a different reaction pathway for the electrochemical reduction of PC versus EC-based electrolytes at graphite electrodes with $LiPF_6$ as the salt in common. We examined the reduction products formed using ex-situ Fourier Transform Infrared (FTIR) spectroscopy in attenuated total reflection (ATR) geometry. The results show the pathway for reduction of PC leads nearly entirely to lithium carbonate as the solid product (and presumably propylene gas as the co-product) while EC follows a path producing a mixture of organic and inorganic compounds. Possible explanations for the difference in reaction pathway are discussed.

---

[*] Electrochemical Society Active Member

[z] Corresponding author e-mail: GVZhuang@lbl.gov

It is well known in the literature that there is a considerable imbalance of cathodic versus anodic total charge for the carbon/graphite negative electrode in a Li-ion battery during the first few (formation) cycles[1]. This charge imbalance or irreversible capacity has been attributed to solvent co-intercalation, electrolyte reduction, SEI layer formation, and other side reactions accompanying intercalation and deintercalation of carbon/graphite electrodes[2]. Most of this irreversible capacity occurs in the potential region > 0.5 V (vs. Li/Li^+), and in the case of graphite can be distinguished from the charge for intercalation/deintercalation which produces three well-defined sharp peaks in the differential capacity curve < 0.5 V (vs. Li/Li^+). These well-defined features are reversible (charge balanced) and correspond to stage I, stage II and stage III intercalation compounds, i.e. $Li_{1/x}C_6$ where x = 1, 2 and 3, respectively[3]. It is also well known that total amount of irreversible capacity is very dependent on both the electrode material, e.g. surface area/particle size, and electrolyte composition, e.g. solvent, co-solvents, salt, film forming additives, and impurities. In particular, it is well known that when propylene carbonate (PC) is used as the primary solvent with common inorganic salts like $LiPF_6$ there is essentially continuous electrolyte reduction with a graphite electrode at ca. 0.9 V (vs. Li/Li^+), accompanied by gassing and graphite exfoliation[4-6]. It is presumed that these processes are due to co-intercalation of PC with Li^+ and subsequent reduction to form gases that cause exfoliation. Graphite electrodes can, however, be electrochemically intercalated with Li ion in PC-based electrolytes with the use of certain salts such as lithium bis-oxalatoborate (LiBOB)[4] or certain additives[7-9]. There is spectroscopic evidence that the LiBOB salt and the additive vinylene carbonate (VC) are electrochemically reduced at potentials above ca. 0.9 V (vs. Li/Li^+) to form a surface

layer that prevents PC co-intercalation. Why solvent co-intercalation and subsequent reduction occurs only with PC and not the chemically closely related solvent ethylene carbonate (EC) or the other non-cyclic esters of carbonic acid, e.g. dimethyl carbonate (DMC) or methylethyle carbonate (EMC), is an active area of scientific inquiry. The dielectric constants of EC and PC are comparable and either classical[10] or modern quantum chemical theories[11] of ion solvation would predict nearly equal energies of Li ion solvation, i.e. if solvent co-intercalation occurs with PC it would expected to occur with EC as well. There are reports using in-situ AFM[12,13] and DEMS[14] that there is ethylene (gas) formation at ca. 0.8 V (vs. Li/Li^+) and some limited exfoliation of graphite anodes in a commonly used EC-based electrolyte, EC:DMC (1:1)/1M $LiClO_4$. Although neither of these studies reported a direct comparison with PC-based electrolytes, it appears that reduction of co-intercalated solvent molecules occurs in both EC-based and PC-based electrolyte, but for some reason the reduction of EC to gas, e.g. ethylene, stops after a short period, whereas the reduction of PC to gas, e.g. propylene, continues unabated.

In the present work, we present results testing the hypothesis that there is a different reaction pathway for the electrochemical reduction of PC versus EC at graphite electrodes. We examined the reduction products formed on commonly used particulate graphite material using ex-situ Fourier Transform Infrared (FTIR) spectroscopy in the attenuated total reflection (ATR) mode. The electrodes were removed from a Swagelok type cell after charging (lithiation) at differing potentials and/or times. The results clearly show there is a different pathway for reduction of PC versus EC on graphite electrodes, the one with PC leading nearly entirely to lithium carbonate as the solid product (and

presumably propylene gas as the co-product) while EC follows a path producing products having a uniquely different components, e.g. poly-oxyethylene and lithium oxalate.

Experimental

The graphite anodes laminated on the 25μm thick copper current collector were composed of 92% MAG-10 graphite (Sumitomo) and 8 wt% PVDF (Kureha) with a loading of 3.64 mg/cm^2 active material. Electrochemical cells were assembled in Ar filled glove box (water and oxygen contents < 10 ppm.). The electrochemical cell were of the Swagelok® type assembled using the graphite anodes (1 cm^2 area), Li reference and counter electrodes, and a Celgard (3501) separator. The electrolytes used were 1.2M $LiPF_6$/ethylene carbonate (EC): ethyl methyl carbonate (EMC) (3:7 wt%) (Quallion) and 1.0m $LiPF_6$/Propylene Carbonate (PC) (Molicell). The graphite anodes were galvanostatically charged/discharged at a low rate of C/25 (50 μAcm^{-2}) using a battery cycler (BT-2043 Arbin cycler, College Station, TX). All the potential reported in this work is referenced to Li/Li$^+$ redox couple.

To examine the potential dependence of the reduction chemistry, the anode was charged (lithium intercalation) from its OCV to various potentials ranging from 1.5 V to 10 mV, held potentiostatically at this potential for two hours, unless otherwise noted in text, then discharged galvanostatically to 1.0 V. A new electrode was used for each holding potential. To avoid possible Li metal deposition, no holding time was applied to the cell charged to 10 mV. The discharge procedure (lithium deintercalation) was applied to avoid further Li-electrolyte reaction during rinsing and spectroscopic analysis. Cells were held at the discharge voltage for 1 hour prior to disassembly in glove box. After allowing the volatile electrolyte component (EMC) to evaporate in the glove box, the

anodes were either transferred directly to He filled spectrometer sample chamber in vacuum carrier for FTIR analysis, or rinsed with dimethyl carbonate (DMC) to remove residual electrolyte before FTIR analysis.

The FTIR spectra were obtained in ATR mode directly on the electrodes surfaces either as-is or after DMC rinsing. In most cases, the EC-$LiPF_6$ precipitate is thicker than the penetration depth of the IR light and attenuates the signal from the surfaces of the graphite particles, i.e. only the spectrum of the precipitate is observed[15]. In some cases, features other than those of the EC-$LiPF_6$ precipitate could be observed, and as we show these features are enhanced by light DMC rinsing to remove the precipitated electrolyte. Most spectra shown and discussed are, however, from rinsed samples, as these are the highest quality spectra. The spectra were acquired with resolution 4 cm^{-1} and total of 512 scans were co-added. Details of our FTIR-ATR analysis have been reported in earlier publications[15, 16].

Results and Discussion

EC-based Electrolyte - Fig. 1a is the differential capacity (dQ/dV) vs. potential of the MAG-10 graphite anode in the first complete charge and discharge cycle in the EC-based electrolyte at a current density of 50 μAcm^{-2}. The three pronounced features at 203 mV, 112 mV and 75 mV in first charging cycle can be attributed to transition between stages in Li-GIC compounds of Li_xC_6, where x varies from 0.17 to 1[3,17]. These features are shifted to 230 mV, 143 mV and 106 mV in the subsequent discharge cycle. The clear sharp peaks with large peak separations due to the well-defined phase transitions indicate a well-ordered graphite structure. On close examination of the potential region above 0.2 V (see Fig.1b), it is found that an additional cathodic peak at 0.75 V is superposed on a

broad and slow varying background, and there are no corresponding anodic processes in this region. The charge passed in this region is usually associated primarily to electrolyte reduction rather than Li-ion intercalation[1]. The total integral charge in each potential region was calculated and summarized in Table.1. The total charge imbalance, a net cathodic excess usually termed "irreversible capacity", is 27.5 % of the discharge (useable) capacity of the anode. About 46% of excess cathodic charge was found to occur between 2V ~ 0.5 V and the rest in the potential region below ca. 0.3 V where Li intercalation into graphite takes place. The results shown in Figure 1 and Table 1 are typical of graphite anodes in EC-based electrolyte[18].

To investigate the SEI formation process at each potential region, a series of nominally identical graphite electrodes were charged galvanostatically to the potentials indicated by A – G in Figure 1, held at the selected potential for 2 hours. Before removed for spectral analysis, those samples charged to < 1 V were discharged to 1 V at the same current density (50 μAcm^{-2}). At cut-off potentials 1.5 V, 1.0 V and 0.75 V, i.e. sample points A-C in Fig.1b, the IR spectra were virtually identical to that from an anode merely soaked in electrolyte at OCV, i.e. no current or potential applied. We have discussed in detail the absorption bands of both the bulk electrolyte and the residual electrolyte (EC solvate) in a previous publication, including complete assignments aided by DFT calculations[15]. Only for samples removed after charging at or below 0.5 V could any new features be observed on an electrode with or without rinsing with DMC. The spectra from sample point H, after the first complete cycle, is an important starting point in the analysis because: a) this sample should have an as-formed SEI layer which is representative of this particular battery chemistry, and b) thus should be used to establish

the procedure, e.g. rinsing-off the residual electrolyte, to analyze samples that are expected to have a less well-formed SEI layer. Figure 2 shows the evolution of the spectra from sample point H with DMC rinsing time. Without rinsing the spectrum is dominated by features entirely from the residual electrolyte (EC solvate), with some new features just barely detectable in the 1650 – 1600 cm^{-1} region. These features become strongly enhanced with DMC rinsing, and it appears that 60 sec. is the optimal time for nearly complete removal of residual electrolyte. This rinsing time was then used as the standard procedure in subsequent experiments.

Figure 3 shows the time dependence of the IR spectra with a holding potential of 0.5 V (point D in Fig.1a). With prolonged holding time at 0.5 V, the DMC-insoluble layer grows thicker as evidenced by the increase in intensity of the 1630 cm^{-1} peak, and appears to reach an equilibrium state at about 10 hr. The total integrated (cathodic) charge during this holding period (including the initial galvanostatic charging to 0.5 V) was ca. 200 $\mu Ah\ cm^{-2}$. The equilibrium states of each sample corresponding to E, F and G in Fig.1a, i.e. at 0.215 V (stage III Li-GIC), 0.13 V (stage II) and 0.01 V (stage I), respectively, all yielded spectra similar to the 10 hr. spectrum in Fig.3, although the time to achieve an invariant spectrum was much shorter. It is important to note that some of the other absorption bands in Fig. 3 increase commensurately with the 1630 cm^{-1} peak, i.e. remain in relatively constant proportionality, with time of holding at the fixed potential. These are essentially all of the C-H region at 2800 – 3000 cm^{-1}, and the bands near 1320, 1070, and 840 cm^{-1}. It is, therefore, reasonable to associate these bands to one another and to the SEI layer on the graphite particles.

For the purposes of discussion, we fit the spectrum (spectrum I, Fig.4) from the sample point H in Fig.1a after 65 seconds DMC washing with scaled (in relative intensities) spectra (spectra II-IV, Fig.4) of reference compounds containing the functional groups having IR bands matching those in the experimental spectrum. This matching is shown in Figure 4 for the region below 2000 cm^{-1} and in Figure 5 for the C-H stretching region around 3000 cm^{-1}. There is clearly some residual EC-solvate even on the rinsed sample H. An important perspective is provided by the reference spectrum from the EC-solvate, namely the relatively weak intensity of the bands in the C-H region to the very strong absorption of the O=C stretching mode near 1800 cm^{-1}. This relative intensity is characteristic of all the alkyl carbonate solvents, EC, DEC, DMC and EMC, as well as most carboxylic acids (at 1650 - 1580 cm^{-1}) and their esters. Therefore, one can easily see that C-H region in spectrum I (Figs. 4 and 5) cannot come *primarily* from any alkyl carbonate or carboxylate, but from another type of C-H-O molecule. The strongest features from sample H not associated with the EC-solvate are near 1660 and 1100 cm^{-1}. These frequencies are characteristic, respectively, of the O=C-O stretching in an oxalate or ester of oxalic acid and the C-O vibration in an alkoxide, such as the lithium methoxide compound shown (not necessarily the best model compound). Lithium oxalate appears to fit the spectrum I in Fig.4 rather well, having a pair of bands matching features at 1630 and 1320 cm^{-1} with about the same relative intensities. The small sharp peak at 1580 cm^{-1}, not always observed in repeat experiments, is possibly from a carboxylate, e.g. lithium propionate. There is only a small amount of lithium carbonate present, as seen from the relatively small peaks at 1480 and 870 cm^{-1}, the latter complicated by contributions from $LiPF_6$ in the solvate. The C-H region is, as we

mentioned above, poorly fitted by lithium methoxide as a model, and the bands around 1070 cm^{-1} appear broader than that in the methoxide as well. The C-H region is much better fitted by model compounds such as polyethylene oxide (PEO) and poly-tetrahydrofuran (THF) (see spectra II and III in Fig. 5), which have, respectively, $(-CH_2CH_2O-)_n$ and $(-CH_2CH_2CH_2CH_2O-)_n$ functionalities. The C-O-C vibration in these polyethers is shifted to slightly higher wavenumbers and is sharper than the C-O vibration in the methoxide, and thus when mixed with an alkoxide would produce an asymmetric band somewhat like that in the anode sample, although not as broad on the lower wavenumber side. It is possible that some of the latter is an artifact of the background subtraction applied to the raw spectrum from the anode, i.e. scattering from rough surface. The relative intensity of the C-H bands to the C-O-C band in the polyethers is reasonably close (within a factor of two) to that in the anode spectrum. It is reasonable to conclude, based on the IR analysis in these experiments, that the passivation film formed on the graphite anode in EC:EMC/$LiPF_6$ after the first formation charge to 0.01 V and discharge to 1.0 V is composed (in descending order of concentration) of compounds chemically similar to lithium oxalate, lithium methoxide, polyethers like PEO or poly-THF, and lithium carbonate.

PC-based electrolyte – The charging curve for the MAG-10 anode in PC based electrolyte had the expected profile shown in the insert to Fig. 6. The electrode clearly could not be intercalated with Li ion in this electrolyte, with the potential remaining at ca. 0.9 V. After 10 hrs. of charging at this condition (500 $\mu Ahcm^{-2}$), the electrode was harvested from the cell and analyzed by ATR-FTIR. The resulting spectrum I, shown in Fig. 6 for the rinsed sample, was remarkably different from that of any sample from the

EC-based electrolyte (see spectrum I in Fig.4). First, features not associated with PC solvate were seen on the sample without rinsing, and the spectrum emerging upon rinsing was very strong and the features well resolved. The spectrum could be easily resolved into two molecular components as shown by the companion spectra from reference compounds, lithium carbonate (Li_2CO_3) (spectrum II) and lithium methoxide (CH_3OLi) (spectrum III). Again, lithium methoxide is only a model compound for the C-O-Li stretching frequency, which fits the strong vibrational band at 1040 cm^{-1} much better here than in the anode charged in EC-based electrolyte. The C-H region in the spectrum of the sample is, however, clearly not fit well by methoxide, so that the specific Li alkoxide, i.e. the R in the generic ROLi, present in the sample is uncertain. Some alkoxide is therefore present in the anodes from both the EC and PC-based electrolytes, but the major difference, and it is a very substantial difference both qualitatively and quantitatively, is the extent of reduction to lithium carbonate in the PC-based electrolyte.

As is now well known, the electrochemical reduction of electrolyte that takes place on graphite anodes is characteristically different in an EC-based electrolyte than in a PC-based electrolyte. What we have added to this body of knowledge from this study is a determination of the difference in chemical nature of the reduction products formed. Working backward from that, together with previous theory and experiment, we attempt in the following to deduce the difference in reaction pathway, and to provide a reasonable explanation for the different reaction paths. We do not contend that the determination of the chemical nature of the reduction product in either electrolyte is definitive, but the *differences* appearing following identical procedures should be illustrative of the *difference* in reaction pathway between EC-based and PC-based electrolyte.

Based on surface chemical compositions of insoluble reaction products deduced from our IR spectra, and the DFT theory of reaction pathways by Balbuena and co-workers[11,19], we suggest the following different reduction paths:

[I] $C_4O_3H_6$ (PC) $+ 2\ e^- + 2\ Li^+ \Rightarrow Li_2CO_3 + CH_3CH{=}CH_2 \uparrow$

versus

[IIa.] $2C_3O_3H_4$ (EC) $+ 2\ e^- + 2\ Li^+ \Rightarrow LiO_2CO(CH_2)_4OCO_2Li$

[IIb.] $LiO_2CO(CH_2)_4OCO_2Li + 2\ e^- + 2\ Li^+$

$\Rightarrow Li_2C_2O_4 + LiOCH_2CH_2OLi + CH_2{=}CH_2 \uparrow$

or

[IIIa] $2C_3O_3H_4$ (EC) $+ 2\ e^- + 2\ Li^+ \Rightarrow LiO_2CO(CH_2)_2OCO_2Li + CH_2{=}CH_2 \uparrow$

[IIIb.] $LiO_2CO(CH_2)_2OCO_2Li + 2\ e^- + 2\ Li^+ \Rightarrow Li_2C_2O_4 + LiOCH_2CH_2OLi$

or

[IIIc.] $n\ \{LiO_2CO(CH_2)_2OCO_2Li\} + 2\ e^- + 2\ Li^+$

$\Rightarrow n\ Li_2C_2O_4 + Li\ [OCH_2CH_2O]_n\ Li$

There is a parallel reaction path of PC to alkoxide, but it is not analogous to reactions [IIb], or [IIIb,c] since lithium oxalate was not observed as co-product. It is possible that the co-product of alkoxide in PC is CO_2 rather than oxalate, due perhaps to the higher electrode potential. It is important to note that all the solid multi-electron reduction products have gaseous co-products. Using graphite electrodes and EC-based electrolyte as here, Lanz and Novak[20] reported ethylene evolution during the first charging half-cycle beginning at a potential of about 0.8 V, with the evolution maximizing at about 0.2 – 0.4 V, but continuing even into the discharging half-cycle. Together with recent AFM observations[12,13], these studies indicate that solvent co-intercalation, solvent reduction

producing ethylene or propylene, and exfoliation all occur in both EC and PC-based electrolytes in the initial reduction process near 0.8 to 1.0 V, but for some reason the exfoliation is more severe with PC and a passivation film never forms, i.e. there is just continuous production of gas and exfoliation of the graphite. The DFT calculations[11,19, 21] clearly show that the Li ion solvation energy plays an important role in determining the electrochemical potential of the first reduction step, [I], [IIa], or [IIIa], and that the solvation energy of EC and PC is not significantly different. From the DFT calculations, the co-intercalation of PC and EC with Li ion would be equally probable, and there is evidence of graphite exfoliation occurring initially in both PC and EC-based electrolytes[14]. To form the alkyl dicarbonate in the co-intercalated state, two alkyl carbonate radical anions formed after ring opening electron transfer have to re-arrange themselves while confined to the graphene interlayer. The DFT calculations were made for gas phase molecules and ions without interaction with a surface or confinement to the graphene interlayer. We suggest that the coupling of the alkyl carbonate radical anions seems to be more likely to occur on the external surface of the graphite because of the rotational and translational motion needed for coupling to occur. Therefore, we suggest that co-intercalated PC or EC molecules are reduced directly to lithium carbonate, propylene and ethylene, respectively, while reduction to the alkyl dicarbonate intermediate occurs only on the external surfaces of graphite particles. In this model, because all multi-electron reductions lead to gas production, reduction on the external surface at potentials above 1.0 V is essential to prevent/halt solvent co-intercalation and consequent gassing and exfoliation. Since lithium oxalate and poly-oxyethylene are products unique to reduction of the EC-based electrolyte, we suggest, by inference, that

these products are the key components of the SEI film and are formed only from reduction processes that occur on the external surface of the graphite particles. We do not, however, offer any explanation as to why reduction of PC, in the model presented above, is apparently only reduced in the co-intercalated state and not on the surface of the graphite particles.

Conclusions

Based on the analysis of graphite electrodes by ex-situ ATR-FTIR spectroscopy, we conclude that the passivation film formed on the graphite anode in EC:EMC/$LiPF_6$ after the first formation charge (C/25 rate) to 0.01 V and discharge to 1.0 V is composed (in descending order of concentration) of compounds chemically similar to lithium oxalate, lithium methoxide, polyethers like PEO or poly-THF, and lithium carbonate. The same electrode clearly could not be intercalated with Li in PC/$LiPF_6$ electrolyte, with the potential remaining at ca. 0.9 V. After 10 hrs. of charging at this condition (500 $\mu Ahcm^{-2}$), the electrode was harvested from the cell and analyzed by ATR-FTIR. The only solid products detected were lithium carbonate and an alkoxide, possibly a mixture of methoxide and ethoxide. Since lithium oxalate and poly-oxyethylene are products unique to reduction of the EC-based electrolyte, we suggest, by inference, that these products are the key components of the SEI film and are formed only from reduction processes that occur on the external surface of the graphite particles. We do not, however, offer any explanation as to why reduction of PC, in the model presented above, is apparently only reduced in the co-intercalated state and not on the surface of the graphite particles.

Acknowledgement

This work was supported by the Office of Advanced Automotive Technologies of the U.S. Department of Energy under contract No. DE-AC03-76SF00098. The authors thank Dr. Yong-Shou Lin of Moli Energy (Canada) Ltd. for supplying PC/$LiPF_6$ electrolyte and Dr. S. -W. Song for performing the initial electrochemistry experiments.

References

1. a) R. fong, U. von Sacken and J. R. Dahn, *J. Electrochem. Soc.*, **137**, 2009 (1990);

   b) J. R. Dahn, T. Zheng, Y. Liu and J. S. Xue, *Science*, **270**, 590 (1995).

2. P. Arora, R. E. White and M. Doyle, *J. Electrochem. Soc.*, **145**, 3647 (1998).

3. J. R. Dahn, *Physical Review B*, **44**, 9170 (1991)

4. K. Xu, S. Zhang, B. A. Poese and T. R. Jow, *Electrochem. Solid-State Lett.,* **5**, A259 (2002).

5. K. Xu, S. Zhang and T. R. Jow, *Electrochem. Solid-State Lett.*, **6**, A117 (2003).

6. M. Masayasu and J.-I. Yamaki, *J. Electroanal. Chem.,* **219**, 273 (1989).

7. B. Simon, J.-P. Boeuve, SAFT, US. Patent # 5,626,981 (1997).

8. H. Ota, K. Shima, M. Ue and J. Yamaki, *Electrochimica Acta*, **49,** 565 (2004).

9. X. Zhang, R. Kostecki, T. J. Richardson, J. K. Pugh and P.N. Ross, *J. Electrochem. Soc.*, **148**, A1341 (2001).

10. B. E. Conway, *Ionic Hydration in Chemistry and Biophysics*, Elsevier/North-Holland, Inc., New York (1981).

11. Y. Wang and P. B. Balbuena, *J. Phys. Chem. B*, **106,** 4486 (2002).

12. S.-K. Jeong, M. Inaba, T. Abe and Z. Ogumi, *J. Electrochem. Soc.*, **148**, A989 (2001).

13. P. Novák, F. Joho, M. Lanz, B. Rykart, J.-C. Panitz, D. Alliata, R. Kötz and O. Haas, *J. Power Sources*, **97-98,** 39 (2001).

14. M. E. Spahr, T. P. Palladino, H. Wilhelm, A. Würsig, D. Goers, H. Buqa, M. Holzapfel and P. Novák, *J. Electrochem. Soc.*, **151**, A1383 (2004).

15. S. -W. Song, G. V. Zhuang and P. N. Ross, Jr., *J. Electrochem. Soc.*, **151**, A1162 (2004).

16. G. V. Zhang and P. N. Ross, Jr., *Electrochem. Solid-State Lett.,* 6, A136 (2003).

17. T. Ohzuku, Y. Iwakoshi and K. Sawai, *J. Electrochem. Soc.*, **140**, 2490 (1993).

18. G. -C. Chung, S.-H. Jun, K.-Y. Lee and M.-H. Kim, *J. Electrochem. Soc.*, **146**, 1664 (1999).

19. Y. Wang, S. Nakamura, M. Ue and P.B. Balbuena, *J. Am. Chem. Soc.*, ***123***, 11708 (2001).

20. M. Lanz and P. Novak, *J. Power Sources*, **102**, 277 (2001).

21. Y. Wang and P. Balbuena, *Int. J. Quantum Chem.*, **102**, 724 (2005).

Table 1. Charge integrated over different potential regions on the charge (intercalation) and discharge (deintercalation) cycles with Mag-10 graphite anodes in EC:EMC (3:7)/$LiPF_6$ electrolyte at current density of 50 μAcm^{-2}.

Potential (V) vs. Li^+/Li	C_{charge} $\mu Ahcm^{-2}$	Potential (V) vs. Li^+/Li	$C_{discharge}$ $\mu Ahcm^{-2}$	Δ $\mu Ahcm^{-2}$	Δ (%)
2.9→0.5	199	0.53→1	25	174	12.6
0.5→0.215	115	0.245→0.53	56	59	4.3
0.215→0.13	249	0.17→0.245	200	49	3.6
0.13→0.01	1192	0.04→0.17	1095	97	7.0
Total	1755		1376	379	27.5

$\Delta = C_{charge} - C_{discharge}$ = "irreversible capacity"

$\Delta(\%) = \Delta/C_{discharge}$

Figure Captions

Figure 1. a) dQ/dV vs. potential (vs. Li/Li^+) of a Mag-10 graphite anode cell in the first complete charge/discharge cycle at 50 μAcm^{-2}; b) expanded scale for dQ/dV between 2.2 V and 0.5 V.

Figure 2. Evolution of FTIR spectra from sample H in Fig.1b, subject to 0 s (I); 20 s (II); 30 s (III); 40 s (IV) and 60 s (V) DMC washing.

Figure 3. FTIR of pristine graphite anode (I) and anodes charged galvanostatically at C/25 to 0.5 V (sample D in fig.1b) holding for 10 mins. (II); 2 hours (III); 10 hours (IV), followed by DMC wash. Offsets are applied towards each spectrum for clarity.

Figure 4. Spectrum (I) from sample point H in Fig.1b after 65 seconds DMC washing and reference compounds: EC/$LiPF_6$ precipitate (II); lithium methoxide ($LiOCH_3$) (III) and lithium oxalate ($Li_2C_2O_4$) (IV).

Figure 5. Spectrum (I) from sample point H in Fig.1b and reference compounds: poly-tetrahydrofuran (poly-THF) (II) and polyethylene oxide (PEO MW. 2000) (III).

Figure 6. FTIR spectra of (I) SEI layer formed on graphite anode after potential reached plateau at ca. 0.9 V vs. Li/Li^+ in 1m $LiPF_6$/ PC, lithium carbonate (Li_2CO_3) (II) and lithium methoxide ($LiOCH_3$) (III). Inset: First galvanostatic charging curve in graphite at C/25 using 1m $LiPF_6$/PC (A) and 1.2 M $LiPF_6$/ EC:EMC (3:7) (A').

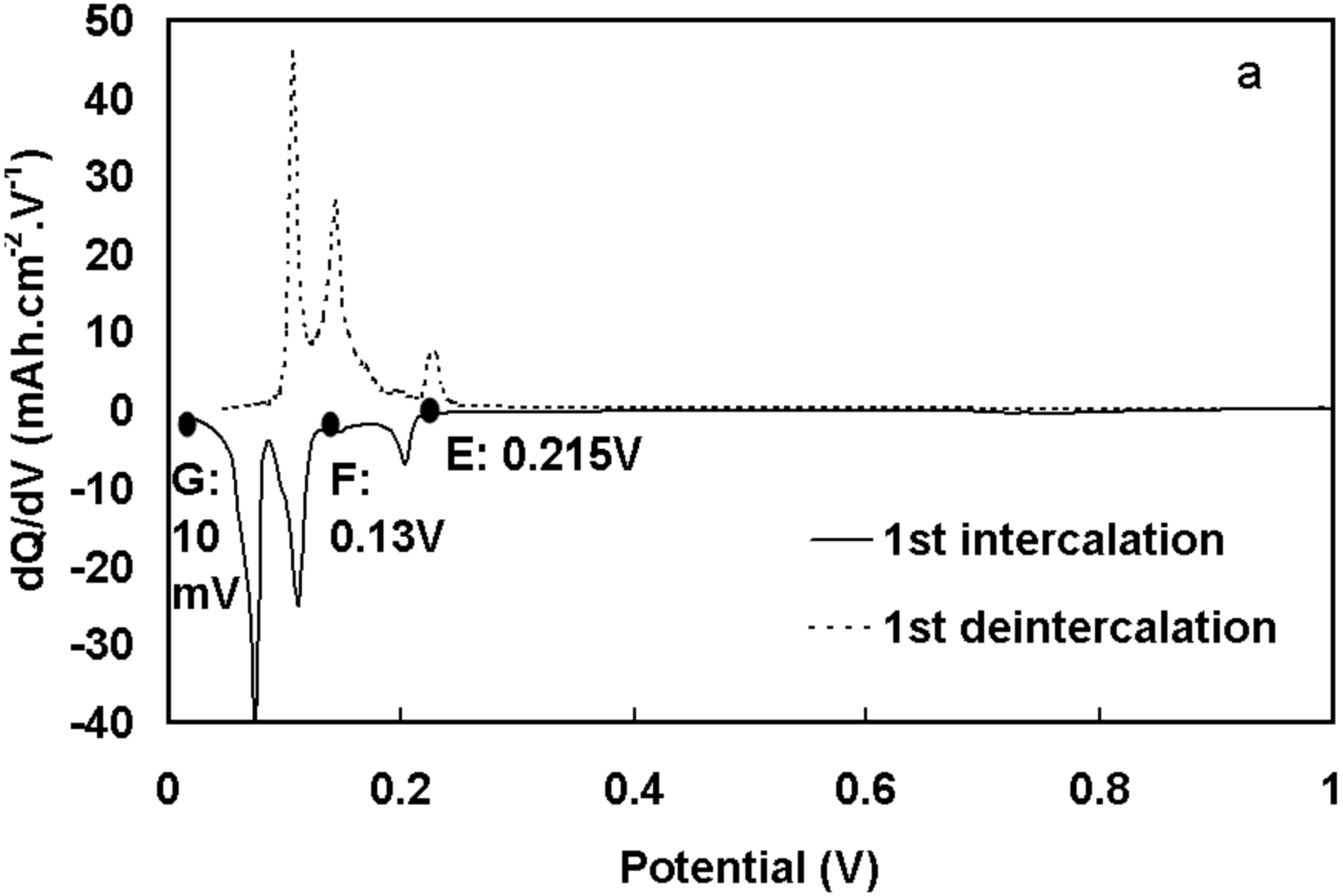
a
dQ/dV (mAh.cm-2.V-1)
50
40
30
20
10
0
-10
-20
-30
-40
0
0.2
0.4
0.6
0.8
1
Potential (V)
G: 10 mV
F: 0.13V
E: 0.215V
1st intercalation
1st deintercalation

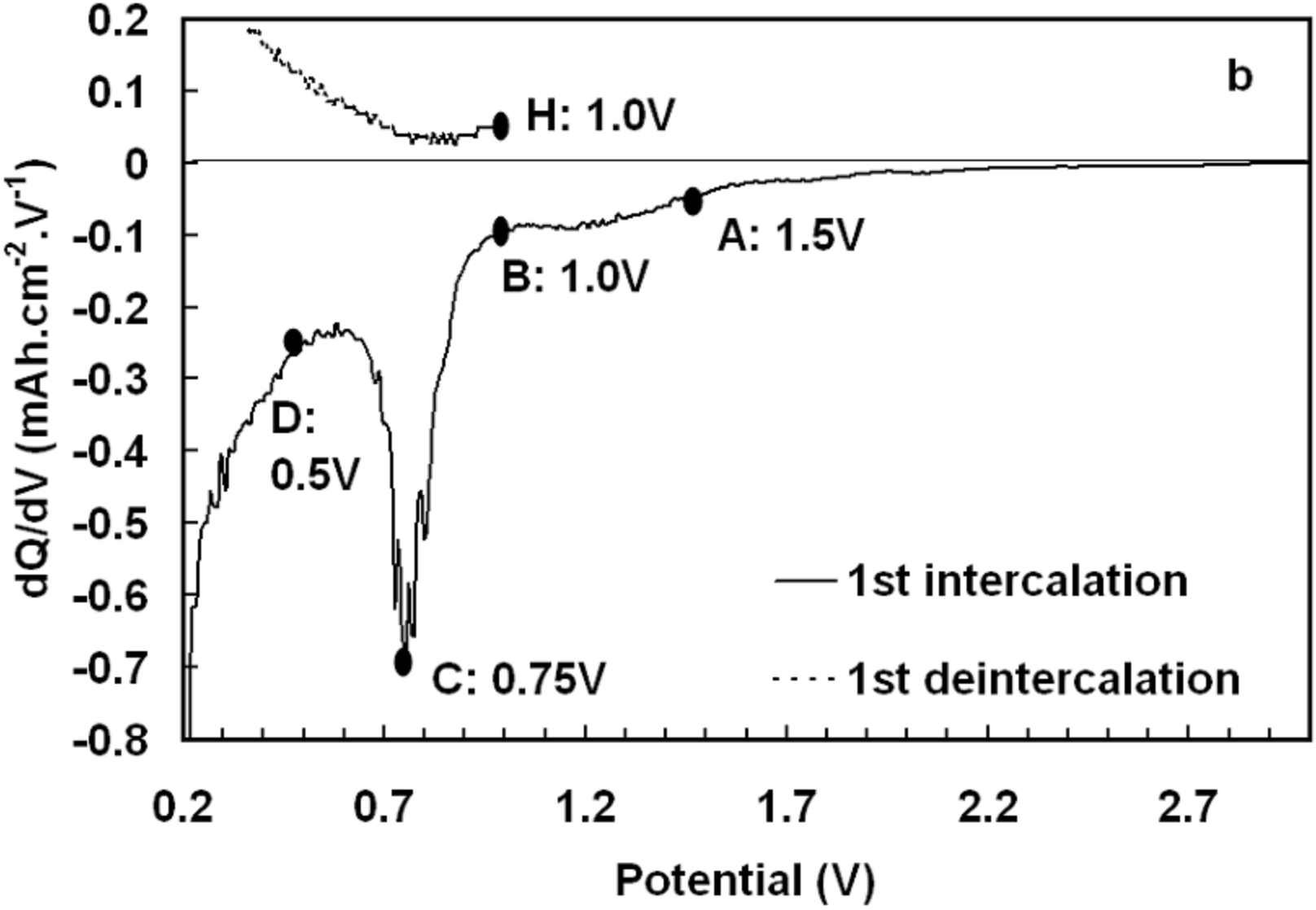
b
H: 1.0V
A: 1.5V
B: 1.0V
D:
0.5V
C: 0.75V
1st intercalation
1st deintercalation
dQ/dV (mAh.cm-2.V-1)
Potential (V)
0.2
0.1
0
-0.1
-0.2
-0.3
-0.4
-0.5
-0.6
-0.7
-0.8
0.2
0.7
1.2
1.7
2.2
2.7

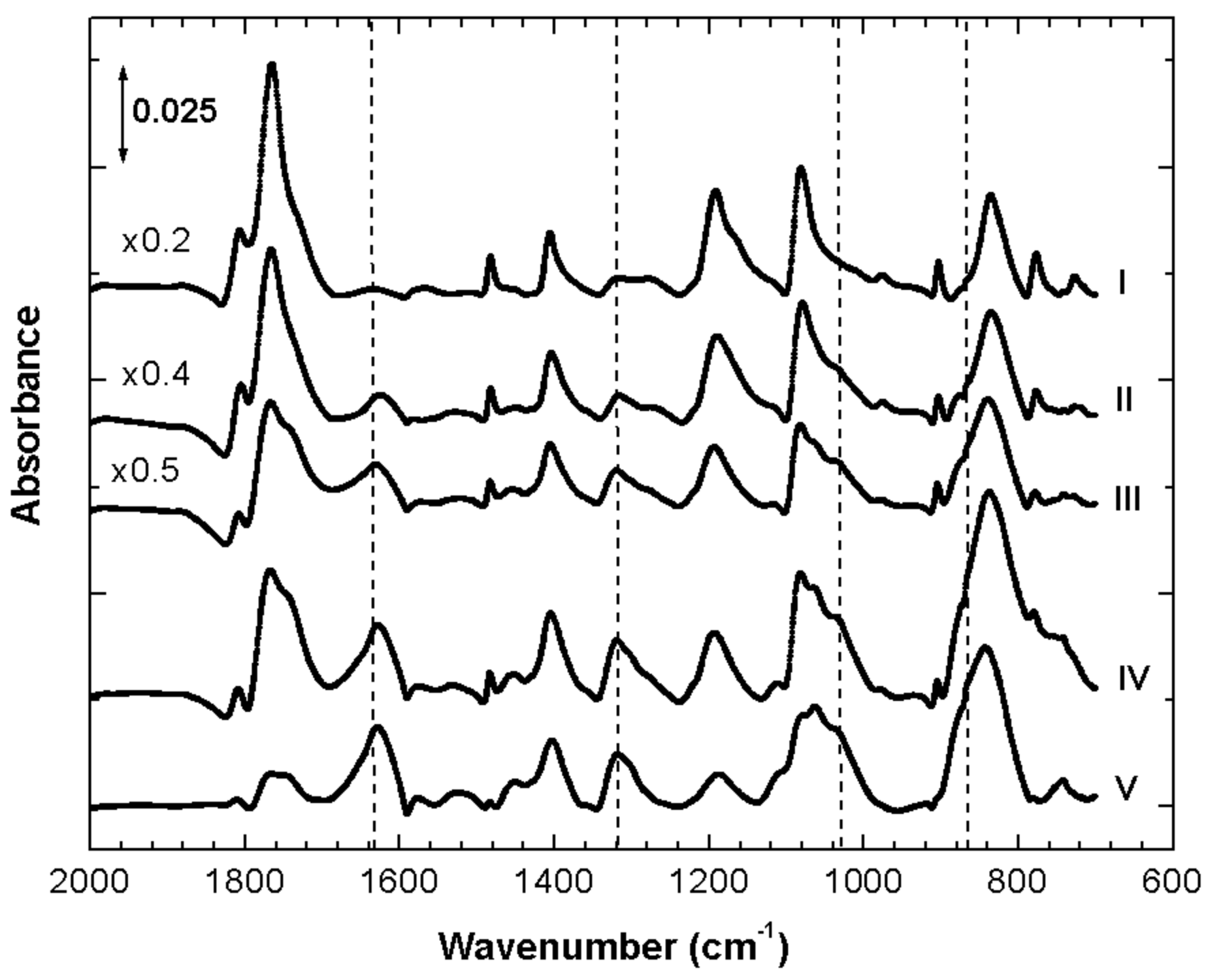
0.025
x0.2
x0.4
x0.5
I
II
III
IV
V
Absorbance
2000
1800
1600
1400
1200
1000
800
600
Wavenumber (cm-1)

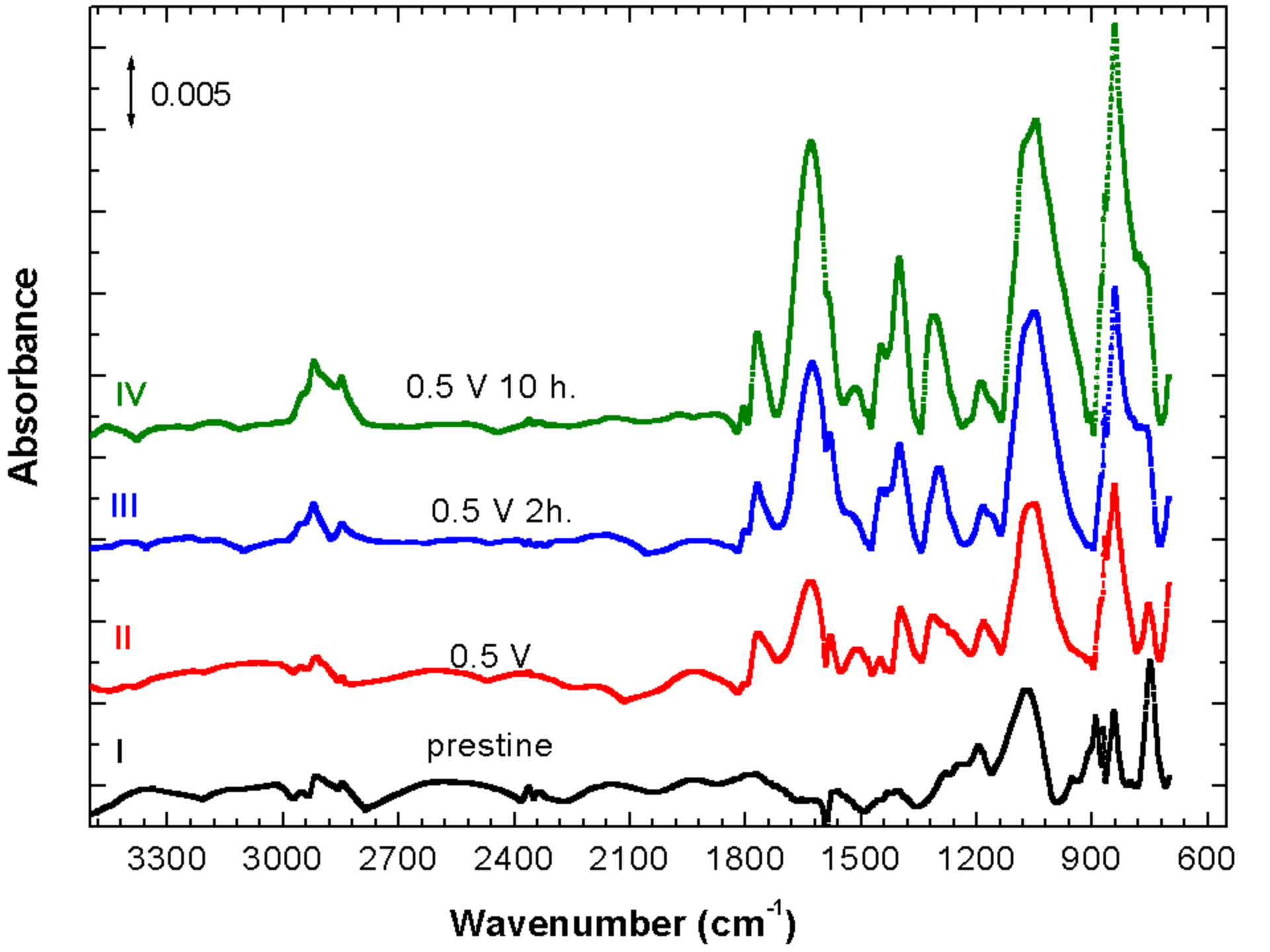
0.005
IV
0.5 V 10 h.
III
0.5 V 2h.
II
0.5 V
I
prestine
Absorbance
3300
3000
2700
2400
2100
1800
1500
1200
900
600
Wavenumber (cm-1)

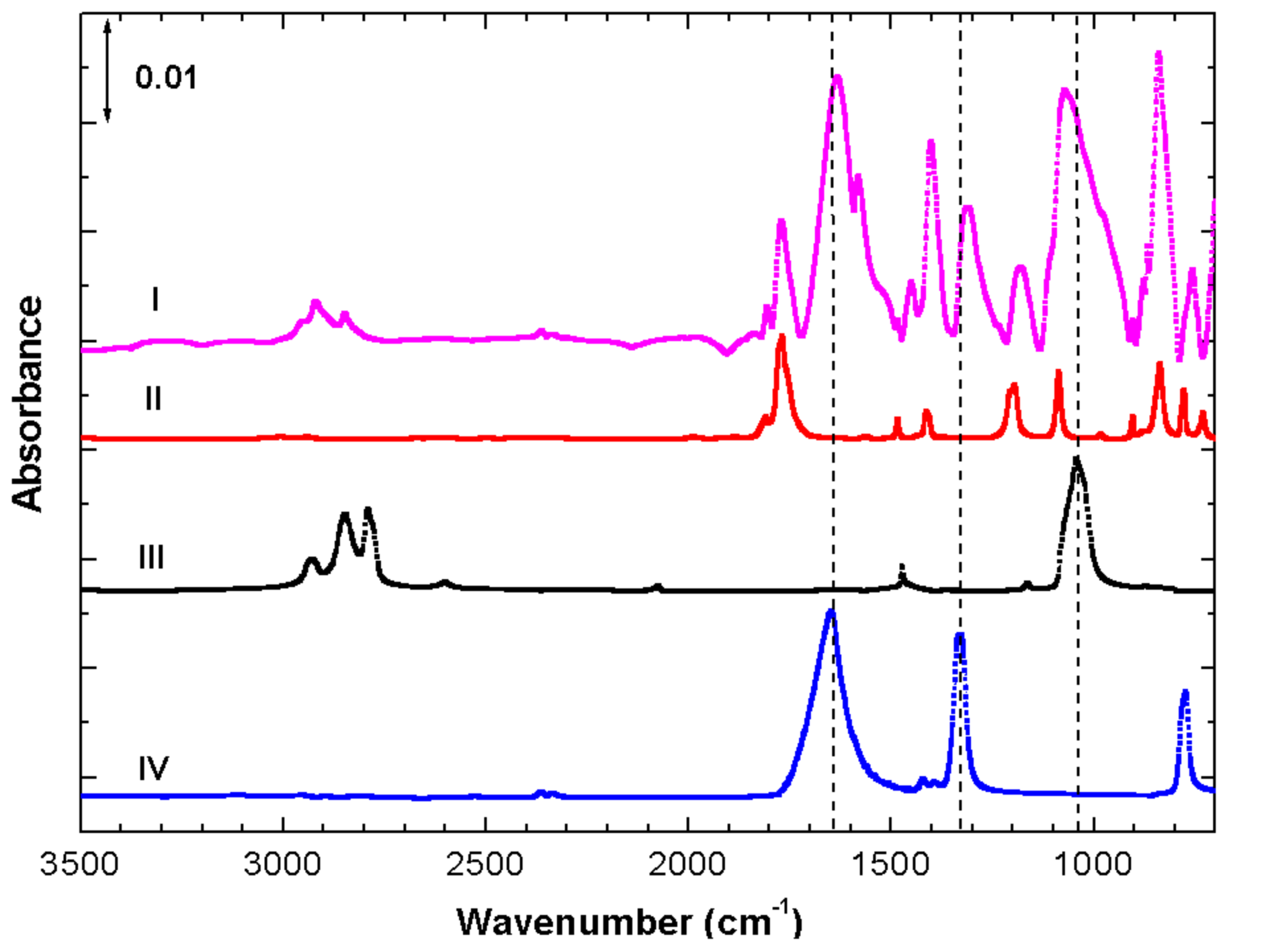
0.01
I
II
III
IV
Absorbance
3500
3000
2500
2000
1500
1000
Wavenumber (cm-1)

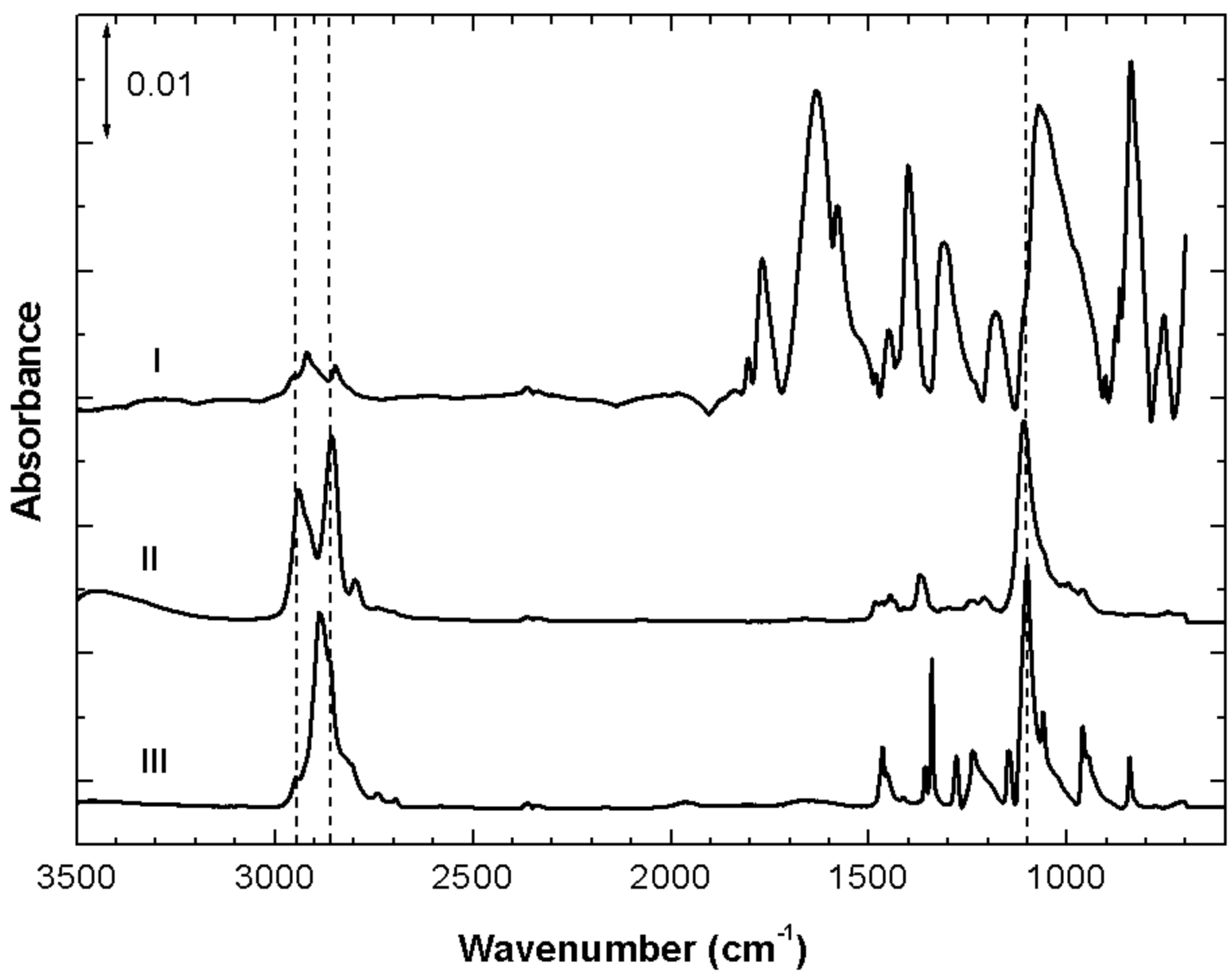
0.01
I
II
III
Absorbance
3500
3000
2500
2000
1500
1000
Wavenumber (cm-1)

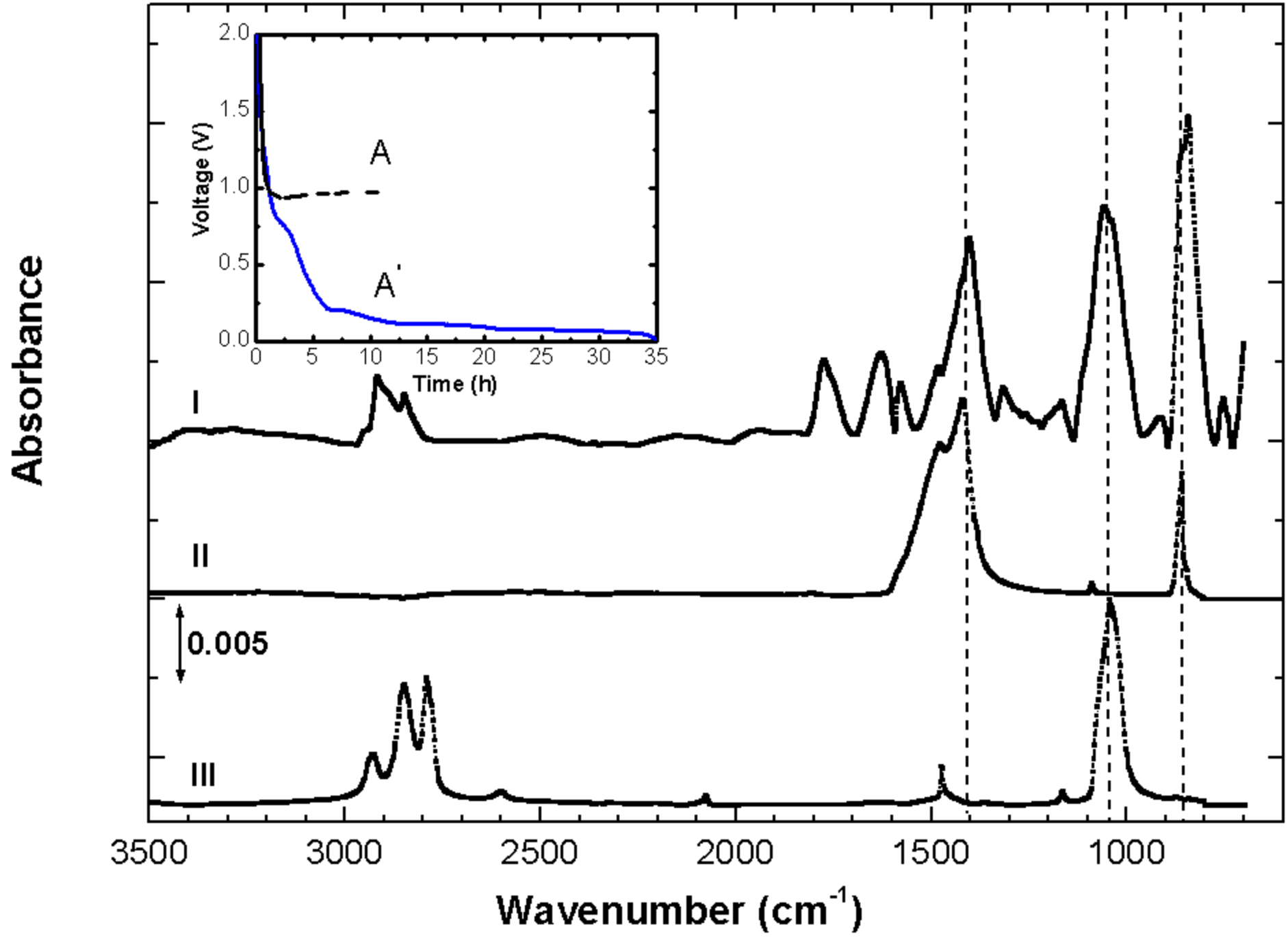
Absorbance
Wavenumber (cm-1)
3500
3000
2500
2000
1500
1000
I
II
III
0.005
Voltage (V)
Time (h)
A
A'
0.0
0.5
1.0
1.5
2.0
0
5
10
15
20
25
30
35